# Multispectral-Fluorescence Imaging as a Tool to Separate Healthy from Disease-Related Lymphatic Anatomy During Robot-Assisted Laparoscopy

Philippa Meershoek*[1,2], Gijs H. KleinJan*[1,2], Matthias N. van Oosterom[1], Esther M.K. Wit[2], Danny M. van Willigen[1], Kevin P. Bauwens[3], Erik J. van Gennep[4], Alexandre M. Mottrie[3,5], Henk G. van der Poel[2], and Fijs W.B. van Leeuwen[1,2]

*[1]Interventional Molecular Imaging Laboratory, Department of Radiology, Leiden University Medical Center, Leiden, The Netherlands; [2]Department of Urology, Netherlands Cancer Institute–Antoni van Leeuwenhoek Hospital, Amsterdam, The Netherlands; [3]Orsi Academy, Melle, Belgium; [4]Department of Urology, Leiden University Medical Center, Leiden, The Netherlands; and [5]Department of Urology, Onze-Lieve-Vrouw Hospital, Aalst, Belgium*

To reduce the invasive nature of extended pelvic lymph node (LN) dissections in prostate cancer, we have developed a multispectral-fluorescence guidance approach that enables discrimination between prostate-draining LNs and lower-limb–draining LNs. **Methods:** In 5 pigs, multispectral-fluorescence guidance was used on da Vinci Si and da Vinci Xi robots. The animals received fluorescein into the lower limb and indocyanine green–nanocolloid into the prostate. **Results:** Fluorescein was detected in 29 LNs (average of 3.6 LNs/template), and indocyanine green–nanocolloid was detected in 12 LNs (average of 1.2 LNs/template). Signal intensities appeared equal for both dyes, and no visual overlap in lymphatic drainage patterns was observed. Furthermore, fluorescein supported both the identification of leakage from damaged lymphatic structures and the identification of ureters. **Conclusion:** We demonstrated that the differences in lymphatic flow pattern between the prostate and lower limbs could be intraoperatively distinguished using multispectral-fluorescence imaging.

**Key Words:** image-guided surgery; prostate cancer; fluorescence; multiplexing; robotic surgery

**J Nucl Med 2018; 59:1757–1760**
DOI: 10.2967/jnumed.118.211888

The metastatic pattern of prostate cancer to the lymphatic system has caused the European Association of Urology to recommend extended pelvic LN dissection for prostate cancer patients who are at intermediate or high risk (i.e., whose estimated risk of nodal metastases exceeds 5% based on the Briganti or Kattan nomogram (*1*)). Unfortunately, extended pelvic LN dissection can damage the natural lymphatic flow in the pelvis and result in an increased complication rate (*2–4*), with lymphoceles (10.3%) and lymphedema (4.1%) being the most common (*5,6*).

Received Mar. 26, 2018; revision accepted May 2, 2018.
For correspondence or reprints contact: Fijs W.B. van Leeuwen, Interventional Molecular Imaging Laboratory, Department of Radiology, Leiden University Medical Center (LUMC), Albinusdreef 2, P.O. Box 9600, Postal Zone C2-S, 2300 RC, Leiden, The Netherlands.
E-mail: f.w.b.van_leeuwen@lumc.nl
*Contributed equally to this work.
Published online May 18, 2018.


For indications such as breast and penile cancer, minimally invasive sampling of the so-called first tumor-draining LNs, that is, sentinel nodes (SNs), has helped reduce the number of patients requiring a LN dissection by more than 75% (*7–9*). However, pelvic SN dissections in intermediate- and high-risk prostate cancer patients is a 1-stop-shop procedure that includes extended pelvic LN dissection, because surgical reexploration of the pelvic nodal basins after SN sampling is cumbersome, and relying solely on SN sampling could leave tumor-bearing non-SNs in situ in 27.1% of LN-positive patients (*7*). This setting creates a demand for technologies that preserve the oncologic outcome of an extended pelvic LN dissection but reduce its impact on healthy lymphatic structures not related to the target organ. When available, such an approach could create a paradigm shift in the surgical treatment of lymphatic disease, changing the focus from "removing nodes that count" to "sparing nodes that are not involved."

We hypothesized that real-time fluorescence multiplexing would allow us to differentiate between the pelvic lymphatic drainage profiles of healthy tissues (lower limb) and primary tumor (prostate) (Fig. 1). We evaluated this concept using the spectrally differentiated lymphangiographic tracer fluorescein and the SN-specific tracer indocyanine green (ICG)–nanocolloid (*10*) during robotic pelvic LN dissections in a porcine model. First, we sought to demonstrate that the ICG-tailored da Vinci fluorescence laparoscopes can also image the clinically approved visible dye fluorescein and support multispectral-imaging applications; second, that multispectral-fluorescence imaging supports real-time intraoperative separation of lower-limb– from prostate-related lymphatic anatomy; and third, that imaging of fluorescein helps visualize damage to the lymphatic network and highlights the ureters.

## MATERIALS AND METHODS

### Camera Setup

The study was performed using 2 generations of a clinical-grade robotic surgical system (da Vinci Si and da Vinci Xi; Intuitive Surgical, Inc.) and its integrated FireFly fluorescence laparoscope. With both generations of the system, the surgical console displays the processed fluorescence signal as artificially colored bright green over a gray-scale background image. Only with the older-generation system (da Vinci Si) is it also possible to display the raw, unprocessed video signal.

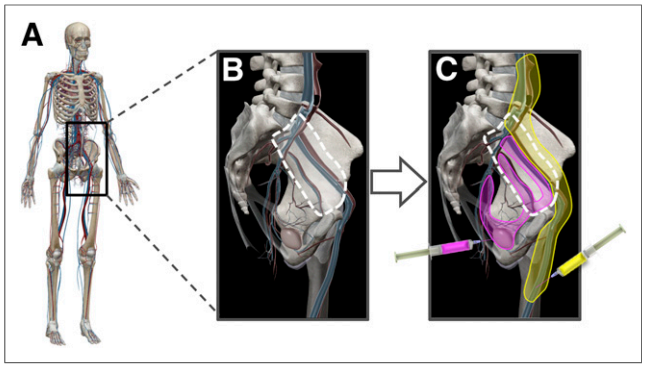


**FIGURE 1.** (A) Schematic representation of relevant anatomical structures, which are highlighted within the box. (B) All lymphatic structures within template (encircled area) are resected during LN resection. (C) Drainage patterns that pass through template are shown for lower limb (yellow area; fluorescein) and prostate (pink area, SNs; ICG-nanocolloid). Images were generated with Visible Body software (Argosy Publishing Inc.).

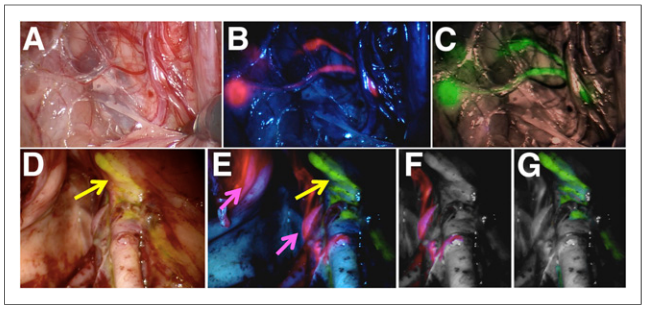


**FIGURE 3.** Multispectral-fluorescence imaging with da Vinci Si system. Shown are lymphatic ducts and 2 SNs containing ICG-nanocolloid on white-light image (A), unprocessed image (ICG, pink) (B), and processed image (ICG, green) (C), as well as lymphatics in external iliac region on white-light image displaying fluorescein-containing lymph duct (yellow arrow) (D), unprocessed multispectral image simultaneously displaying ICG-stained SN (pink arrows) and fluorescein-stained lymph duct (yellow arrow) (E), and images digitally separating the 2 signals into ICG (F) and fluorescein (G).

### Preclinical Evaluation Setup

The multispectral-fluorescence imaging setup was evaluated in 5 male pigs during surgical training (Orsi Academy). The studies were allowed by the Ethical Committee for animal experiments of Gent University (EC2015-152).

To identify the lymphatic drainage of the lower limbs, each animal received 5 mL of a 100 mg/mL solution of fluorescein: 2.5 mL subcutaneously and 2.5 mL intramuscularly into the right hind leg (pigs 1 and 2) or 1.25-mL deposits in both hind legs (pigs 3–5) (Fig. 1). After the fluorescein injection (after 70–150 min) but before the ICG-nanocolloid injection, the pelvic area was evaluated for fluorescein-positive LNs using both white-light and fluorescence imaging.

ICG-nanocolloid was used for lymphatic mapping of the prostate. This tracer was prepared using a modification of a previously described procedure (*11*), resulting in a 2-mL solution with a 0.125 mg/mL concentration of ICG, and was injected intraoperatively using a 2-mL syringe attached to an injection needle by flexible tubing. After insertion of the syringe, the surgeon placed 2–4 tracer deposits into the prostate using the robotic arms (Figs. 1 and 2). After the ICG-nanocolloid injection, the pelvic area was examined for both tracers during a 15- to 30-min period.

## RESULTS

### Fluorescein Imaging Versus ICG-Nanocolloid Imaging

The processed images from both the da Vinci Si and the da Vinci Xi displayed the fluorescence signal of both fluorescein and

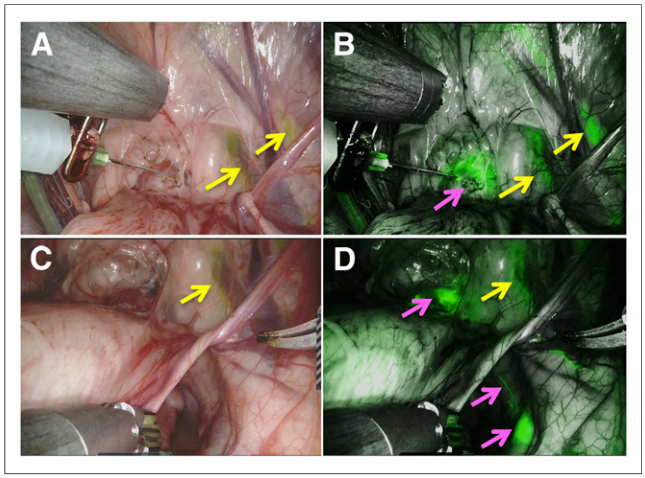


**FIGURE 2.** Multispectral-fluorescence imaging with da Vinci Xi system. During intraprostatic administration of ICG-nanocolloid, white-light image (A) shows fluorescein, whereas fluorescence image (B) shows both fluorescein and ICG. After lymphatic drainage of ICG-nanocolloid, white-light image (C) shows fluorescein-positive areas (yellow arrow), whereas fluorescence image (D) clearly depicts ICG-draining lymphatic duct and SN (pink arrows).

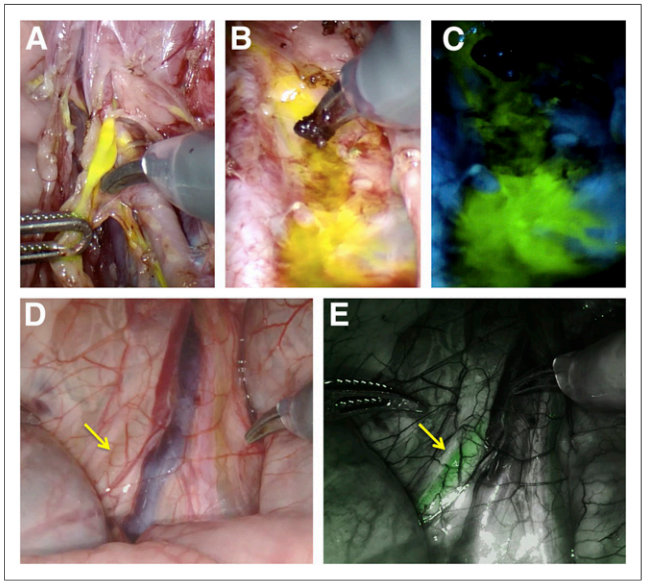


**FIGURE 4.** Additional value offered by fluorescein use. (A) Surgical damage of fluorescein-containing lymph duct (da Vinci Si system). (B and C) Leakage of fluorescein from lymphatics consequent to damage, staining surgical field in white-light mode (B) and fluorescence mode (C). (D and E) Fluorescein-containing ureter (arrows; da Vinci Xi system) as seen in white-light mode (D) and fluorescence mode (E).

**TABLE 1**
Overview of Findings

| Parameter | da Vinci Si | | | da Vinci Xi | | Average |
|---|---|---|---|---|---|---|
| | 2 | 3 | 4 | 1 | 5 | |
| Time between fluorescein injection and intraoperative imaging (min) | 150 | 80 | 92 | 145 | 70 | 107 |
| Massage of fluorescein injection site required for detection? | Yes | NA | NA | NA | NA | — |
| Recording of unprocessed images? | Yes | Yes | Yes | No | No | — |
| Which leg injected with fluorescein? | R | L + R | L + R | R | L + R | — |
| Fluorescein visualization of ureter? | Yes | NE | NE | Yes | Yes | — |
| Fluorescein visualization of lymphatic ducts? | Yes | Yes | Yes | Yes | Yes | — |
| No. of LNs seen with fluorescein | 3 R | 2 L/3 R | 5 L/4 R | 5 R | 4 L/3 R* | 3.6 L/3.6 R* |
| ICG-nanocolloid visualization of lymphatic ducts? | Yes | Yes | Yes | Yes | Yes | — |
| No. of SNs seen with ICG-nanocolloid | 2 L/1 R | 1 L/1 R | 1 L/1 R | 2 L/1 R | 1 L/1 R | 1.4 L/1.0 R* |

*Per leg/template.
NA = not applicable; NE = not evaluated.

ICG-nanocolloid as green (Fig. 2). Differentiation between the 2 types of fluorescence signal required either use of the white-light images to define the location of the fluorescein or use of sequential administration and imaging of fluorescein and ICG-nanocolloid. With the da Vinci Si, the ability to use the unprocessed images, which display the fluorescein signal as yellow/green and the ICG signal as red/pink, made differentiation between the signals much more straightforward (Fig. 3).

### In Vivo Experiments

During surgery (~2 h after injection), fluorescein was detectable in leg-draining LNs (3.6 LNs/template) in the white-light images but was more easily defined in the fluorescence setting (Figs. 2 and 3). Fluorescein leakage provided a valuable indicator of surgical damage to fluorescein-containing lymphatics (Fig. 4). Further, the biologic (renal) clearance of fluorescein supported fluorescence-based visualization of the ureters (Fig. 4) (*12*). In the fluorescence setting, prostate-draining SNs (1.2 SNs/template) and lymphatic ducts became visible within minutes after administration of ICG-nanocolloid. Like the clinically used ICG-$^{99m}$Tc-nanocolloid (*10*), ICG-nanocolloid did not contaminate the surgical field when lymphatic resections were performed.

A clear dividing line in lymphatic drainage pattern was observed between the prostate and the lower limbs, with no signal overlap between the lymphatic drainage profiles of the 2 dyes (Table 1). Differentiation could even occur in the same template (Fig. 3).

## DISCUSSION

To our knowledge, this study was the first to demonstrate the fluorescein and multispectral-imaging capabilities of the da Vinci Si and da Vinci Xi robots. This technology successfully distinguished between ICG-nanocolloid– and fluorescein-positive lymphatics. Despite the theoretic advantages of near-infrared dyes, both dyes could be clearly visualized in vivo (Figs. 2 and 3). With this multispectral-guidance concept, healthy lymphatic structures could potentially be spared, with a consequent reduction in lymphedema of the lower limbs. The fact that commercially available and clinically approved robotic systems allow such a multispectral-imaging approach facilitates the translational aspect of these studies. Further clinical follow-up studies are needed to validate the impact of the proposed imaging concept on the outcomes of clinical trials.

Besides visualizing the lymphatic drainage patterns of the lower limbs, fluorescein imaging also helped detect damage to these same lymphatics; a similar contamination was reported in studies that used free ICG (*13*). In line with the literature, the ureters could also be visualized during surgery using fluorescein (Fig. 4) (*14*).

Combined with previous reports (*10,15,16*), the favorable in vivo visualization of fluorescein using the da Vinci robotic platform again debates the monopoly of near-infrared approaches in the field of fluorescence-guided surgery.

## CONCLUSION

The multispectral-imaging properties of the fluorescence laparoscopes of the da Vinci robotic platform helped realize intraoperative differentiation between prostate-related lymphatic structures (ICG-nanocolloid) and lower-limb–related lymphatic structures, lymphatic damage, and ureters (fluorescein). With that realization, a technology has become available that supports further improvement of the balance between cure and surgically induced side effects.

## DISCLOSURE

Kevin Bauwens and Alexandre Mottrie are affiliated with Orsi Academy. This research was financially supported by an NWO-STW-VIDI grant (STW BGT11272) and a European Research Council grant (2012-306890). No other potential conflict of interest relevant to this article was reported.

## ACKNOWLEDGMENTS

We thank Nikolaos Grivas from the Netherlands Cancer Institute–Antoni van Leeuwenhoek Hospital for his support and assistance.

## REFERENCES


1. Briganti A, Larcher A, Abdollah F, et al. Updated nomogram predicting lymph node invasion in patients with prostate cancer undergoing extended pelvic lymph node dissection: the essential importance of percentage of positive cores. *Eur Urol.* 2012;61:480–487.
2. Geppert B, Persson J. Robotic infrarenal paraaortic and pelvic nodal staging for endometrial cancer: feasibility and lymphatic complications. *Acta Obstet Gynecol Scand.* 2015;94:1074–1081.
3. Todo Y, Yamazaki H, Takeshita S, et al. Close relationship between removal of circumflex iliac nodes to distal external iliac nodes and postoperative lower-extremity lymphedema in uterine corpus malignant tumors. *Gynecol Oncol.* 2015; 139:160–164.
4. Yamazaki H, Todo Y, Takeshita S, et al. Relationship between removal of circumflex iliac nodes distal to the external iliac nodes and postoperative lower-extremity lymphedema in uterine cervical cancer. *Gynecol Oncol.* 2015;139:295–299.
5. Briganti A, Chun FK, Salonia A, et al. Complications and other surgical outcomes associated with extended pelvic lymphadenectomy in men with localized prostate cancer. *Eur Urol.* 2006;50:1006–1013.
6. Clark T, Parekh DJ, Cookson MS, et al. Randomized prospective evaluation of extended versus limited lymph node dissection in patients with clinically localized prostate cancer. *J Urol.* 2003;169:145–147.
7. Wit EMK, Acar C, Grivas N, et al. Sentinel node procedure in prostate cancer: a systematic review to assess diagnostic accuracy. *Eur Urol.* 2017;71:596–605.
8. Wawroschek F, Vogt H, Wengenmair H, et al. Prostate lymphoscintigraphy and radio-guided surgery for sentinel lymph node identification in prostate cancer: technique and results of the first 350 cases. *Urol Int.* 2003;70:303–310.
9. Holl G, Dorn R, Wengenmair H, Weckermann D, Sciuk J. Validation of sentinel lymph node dissection in prostate cancer: experience in more than 2,000 patients. *Eur J Nucl Med Mol Imaging.* 2009;36:1377–1382.
10. van den Berg NS, Buckle T. KleinJan GH, van der Poel HG, van Leeuwen FWB. Multispectral fluorescence imaging during robot-assisted laparoscopic sentinel node biopsy: a first step towards a fluorescence-based anatomic roadmap. *Eur Urol.* 2017;72:110–117.
11. Brouwer OR, Buckle T, Vermeeren L, et al. Comparing the hybrid fluorescent-radioactive tracer indocyanine green-$^{99m}$Tc-nanocolloid with $^{99m}$Tc-nanocolloid for sentinel node identification: a validation study using lymphoscintigraphy and SPECT/CT. *J Nucl Med.* 2012;53:1034–1040.
12. van Leeuwen FW, Hardwick JC, van Erkel AR. Luminescence-based imaging approaches in the field of interventional molecular imaging. *Radiology.* 2015;276: 12–29.
13. Nguyen DP, Huber PM, Metzger TA, Genitsch V, Schudel HH, Thalmann GN. A specific mapping study using fluorescence sentinel lymph node detection in patients with intermediate- and high-risk prostate cancer undergoing extended pelvic lymph node dissection. *Eur Urol.* 2016;70:734–737.
14. Udshmadshuridze NS, Asikuri TO. Intra-operative imaging of the ureter with sodium fluorescein [in German]. *Z Urol Nephrol.*1988;81:635–639.
15. van Willigen DM, van den Berg NS, Buckle T, et al. Multispectral fluorescence guided surgery: a feasibility study in a phantom using a clinical-grade laparoscopic camera system. *Am J Nucl Med Mol Imaging.* 2017;7:138–147.
16. Buckle T, van Willigen DM, Spa SJ, et al. Tracers for fluorescence-guided surgery: how elongation of the polymethine chain in cyanine dyes alters the pharmacokinetics of a dual-modality c[RGDyK] tracer. *J Nucl Med.* 2018;59:986–992.